1. Appendix: The cos Files

In the following we show results for a function that can easily be studied by hand for the various methods under consideration, yet can already illustrate many of the relevant points. We use an approximation of the function $\cos(x)$ by its power series of order 60; so

$$f(x) = \sum_{i=0}^{30} (-1)^i \frac{x^{2i}}{(2i)!}.$$

For the domain $[0, 4\pi]$, this power series represents the cos function to an accuracy of better than 10^{-15}, which is sufficient for work in conventional double precision. Although of course this is one of the worst ways to obtain validated bounds for the cos function, this function is useful for comparisons of bounding methods because it has the following useful features:

(1) Properties of the function are well known
(2) Dependency increases with x from very small to very large
(3) Periodicity allows the study of the same functional behavior with various amounts of dependency
(4) Study at points with both non-stationary and stationary points is possible

The results are shown for the expansion points $x_0 = n \cdot \pi/4$ for $n = 0, ..., 16$. For each of these points, domains are chosen as $x_0 + [-2^{-j}, 2^{-j}]$ for $j = 1, ..., 8$. For each of the values of j, we show relative overestimation $q =$ (computed range - true range) /(true range) as well as the empirical approximation order (EAO) calculated as $1 + \log_2(q_j/q_{j+1})$ for the various methods. EAOs are only calculated until the floor of machine precision is used. We also compute the average empirical approximation order (AEAO) of each method, calculated as the average over j of the EAOs. In all figures, the left shows the results obtained by TM without LDB, i.e. only with direct interval evaluation of the Taylor polynomial, and the right shows the results using LDB.

As expected, the advantage of TM increases with both x_0 and j and reaches up to 16 orders of magnitude for the non-stationary cases in which the linear dominated bounder LDB is applicable, and 5 orders of magnitude for the stationary cases where it is not applicable. In general, the behavior of the high order TM depends mostly on the Taylor polynomial, which is the same except for the signs of coefficients for the families $P_1 = \{0, \pi, 2\pi, 3\pi, 4\pi\}$, $P_2 = \{\pi/2, 3\pi/2, 5\pi/2, 7\pi/2\}$ and $P_3 = \{\pi/4, 3\pi/4, 5\pi/4, ..., 15\pi/4\}$. Interval, MF, and CF as well as low order TM eventually suffer from the dependency problem. High order TM significantly alleviate the dependency problem. For elements of P_1, the collection of all stationary points, the LDB bounder does not offer any benefit over direct interval evaluation of the Taylor polynomial; still the higher order TM methods provide significantly sharper bounds than CF and MF because of the ability to suppress the dependency problem. For elements of P_2 and P_3, LDB provides additional significant improvements in sharpness.

Exercise 1. *There are a few interesting results:*

(1) *Why does the TM convergence order without LDB for elements of P_2 exceed that of CF, but it does not do this for elements of P_3?*
(2) *Why does the TM convergence order for the elements in P_1 exceed that of CF and MF?*

(3) *Why does it exceed it by* 2*?*
(4) *How does the behavior of TM at stationary points generalize to various obvious multidimensional extensions of the example?*

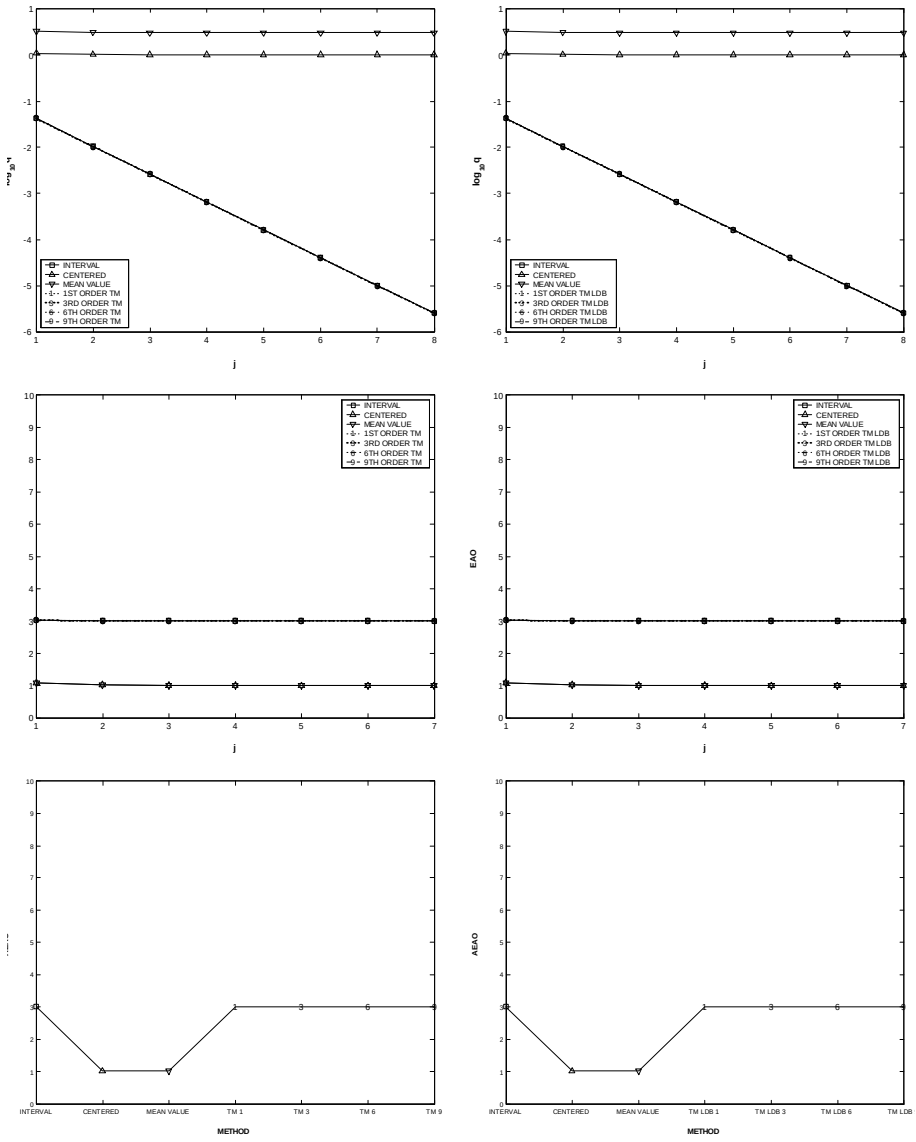

FIGURE 1. At the expansion point $x_0 = 0$.

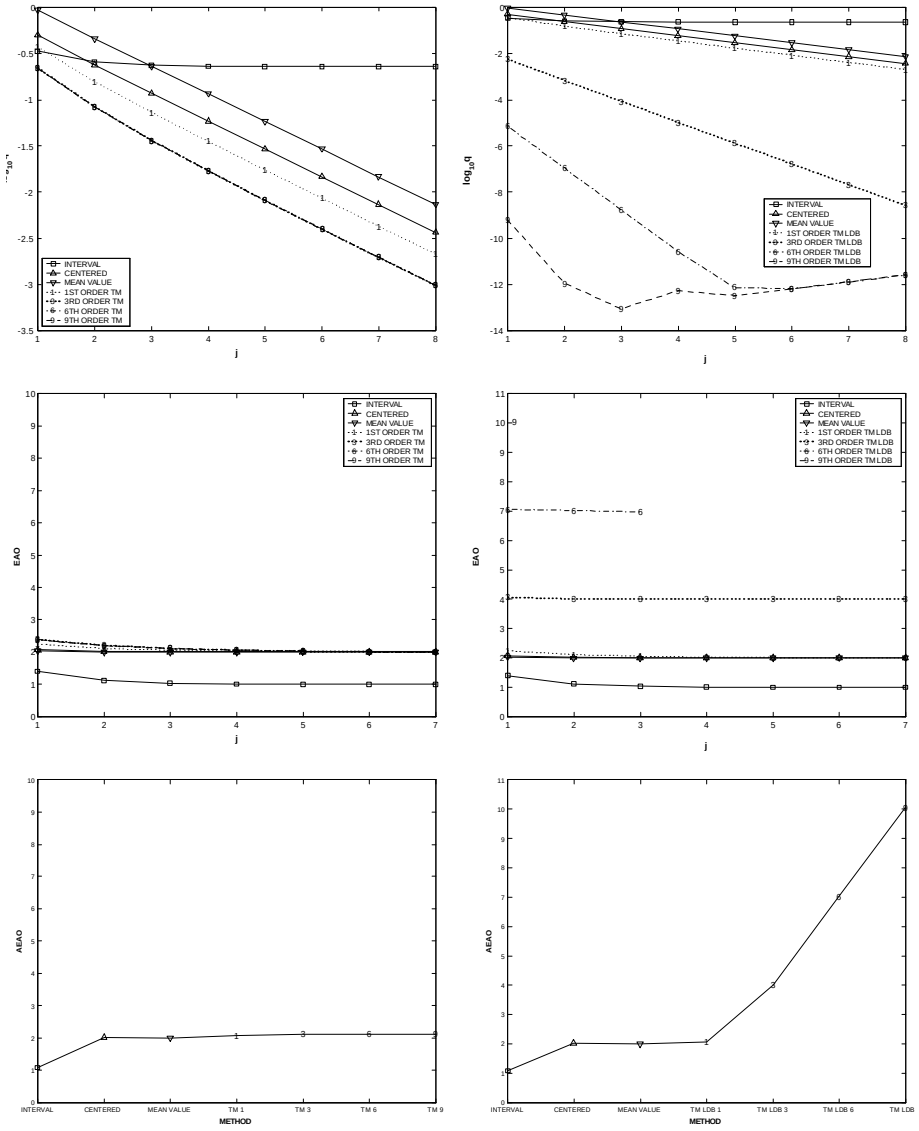

FIGURE 2. At the expansion point $x_0 = \pi/4$.

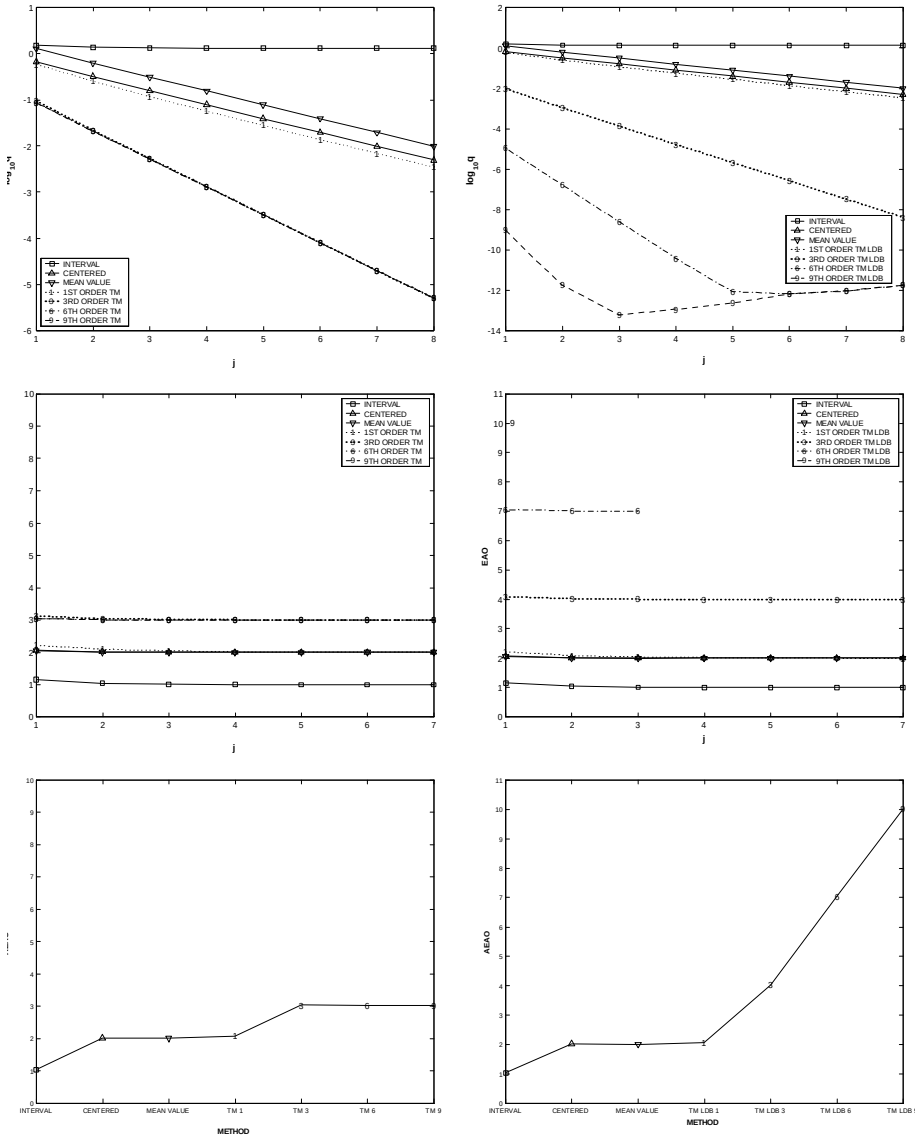

FIGURE 3. At the expansion point $x_0 = \pi/2$.

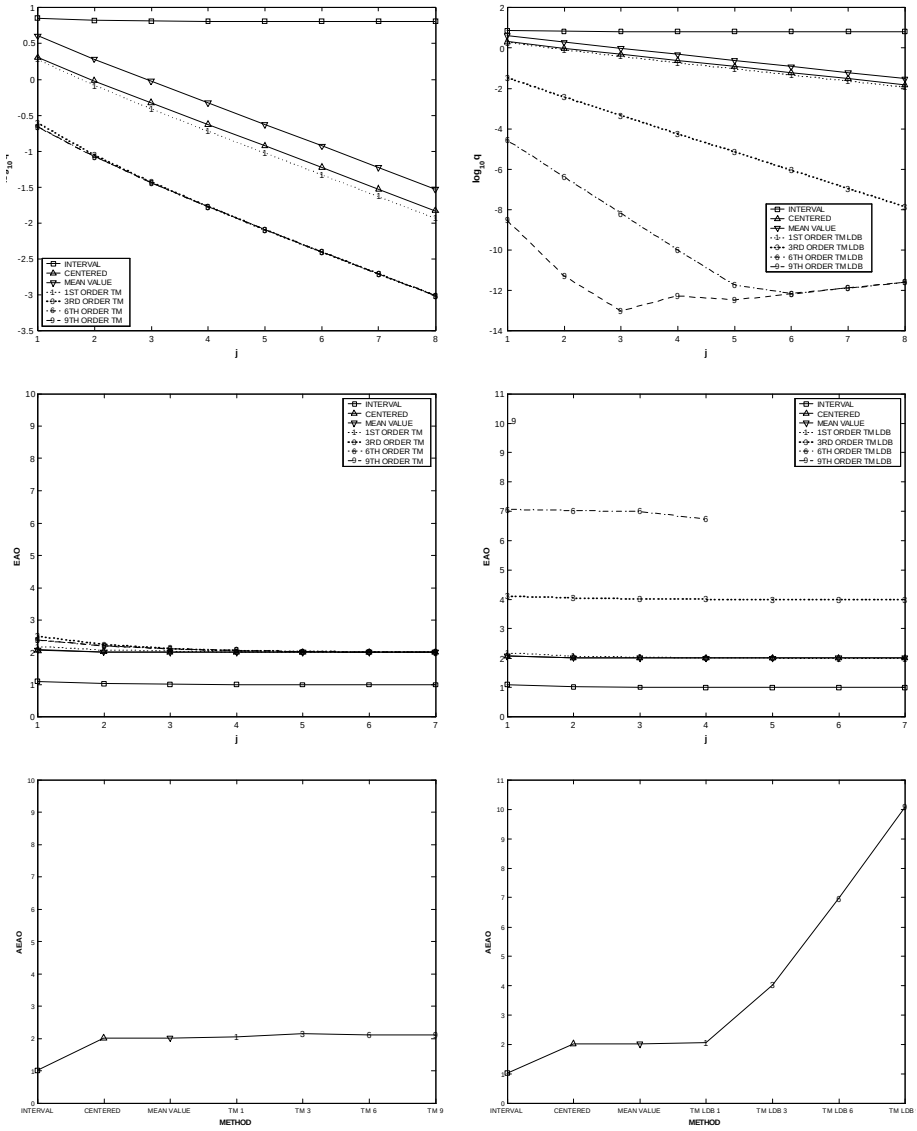

FIGURE 4. At the expansion point $x_0 = 3\pi/4$.

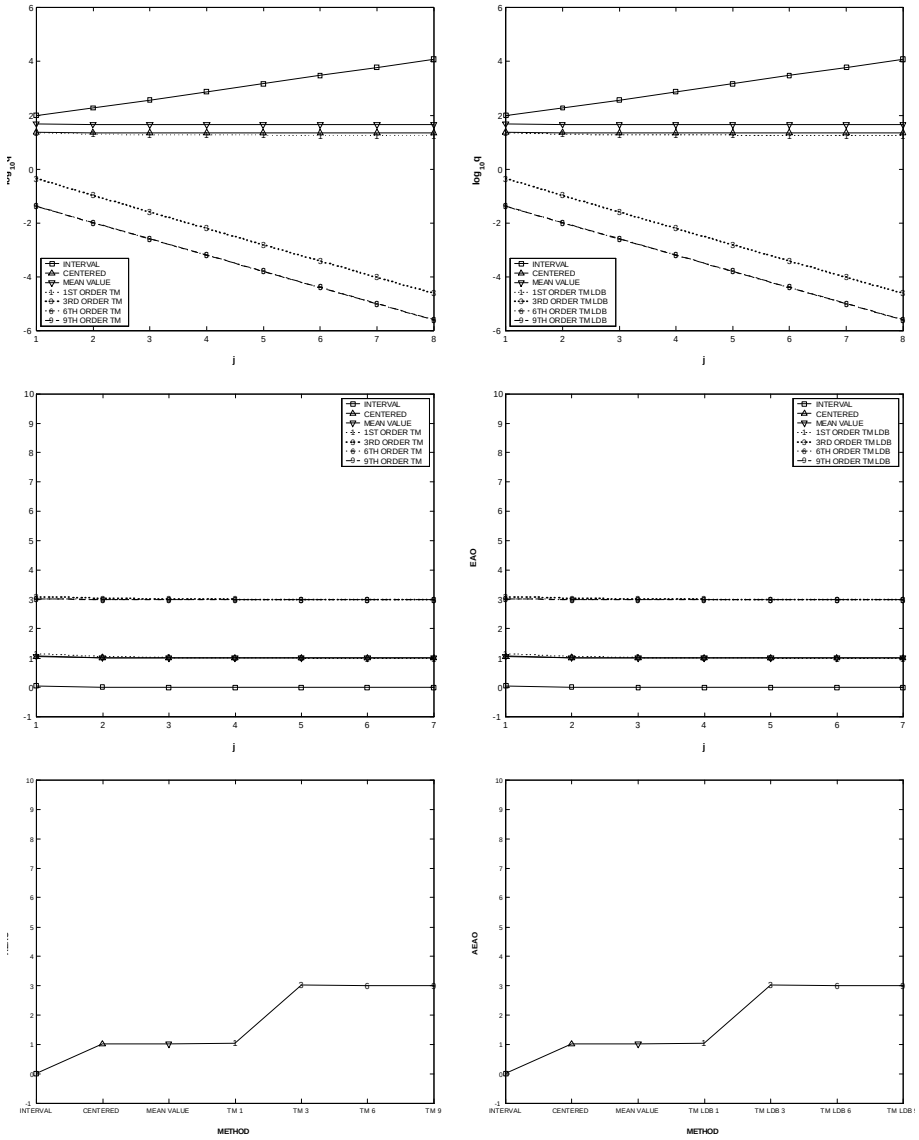

FIGURE 5. At the expansion point $x_0 = \pi$.

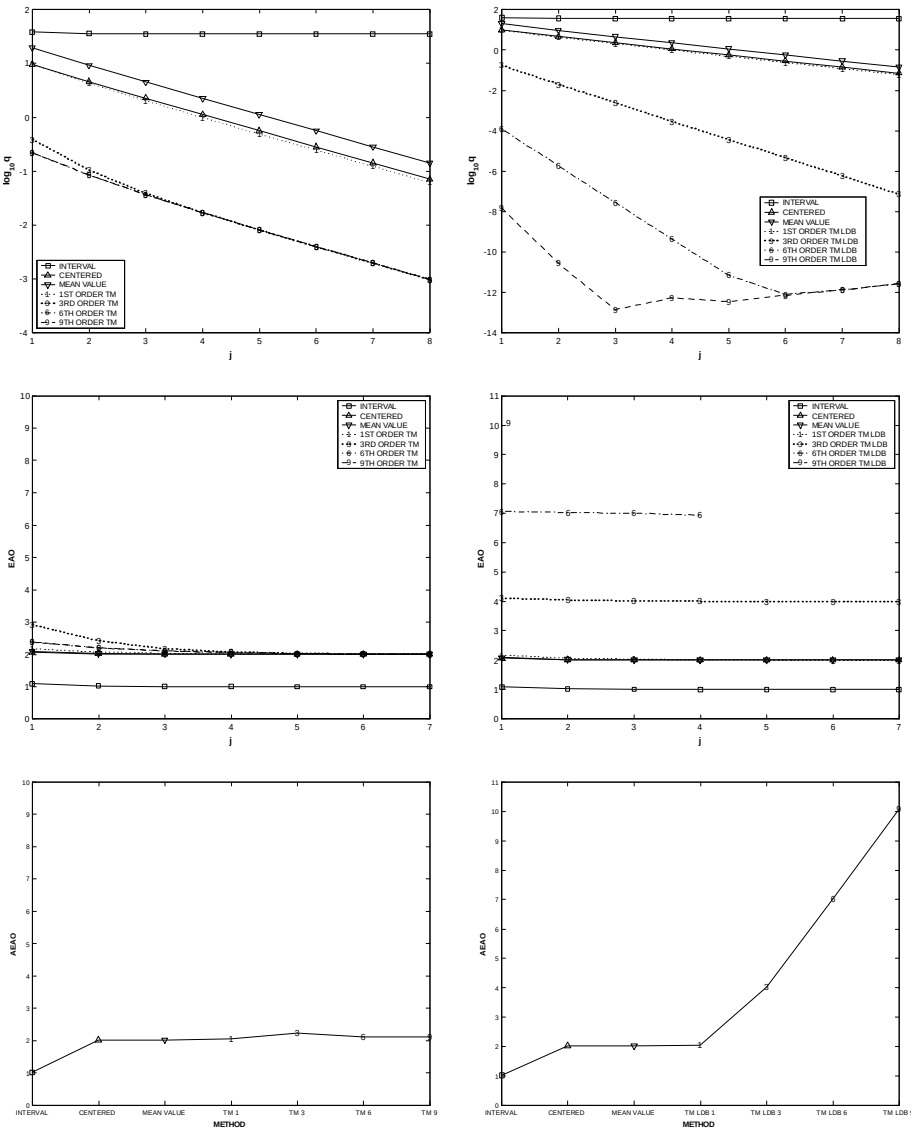

FIGURE 6. At the expansion point $x_0 = 5\pi/4$.

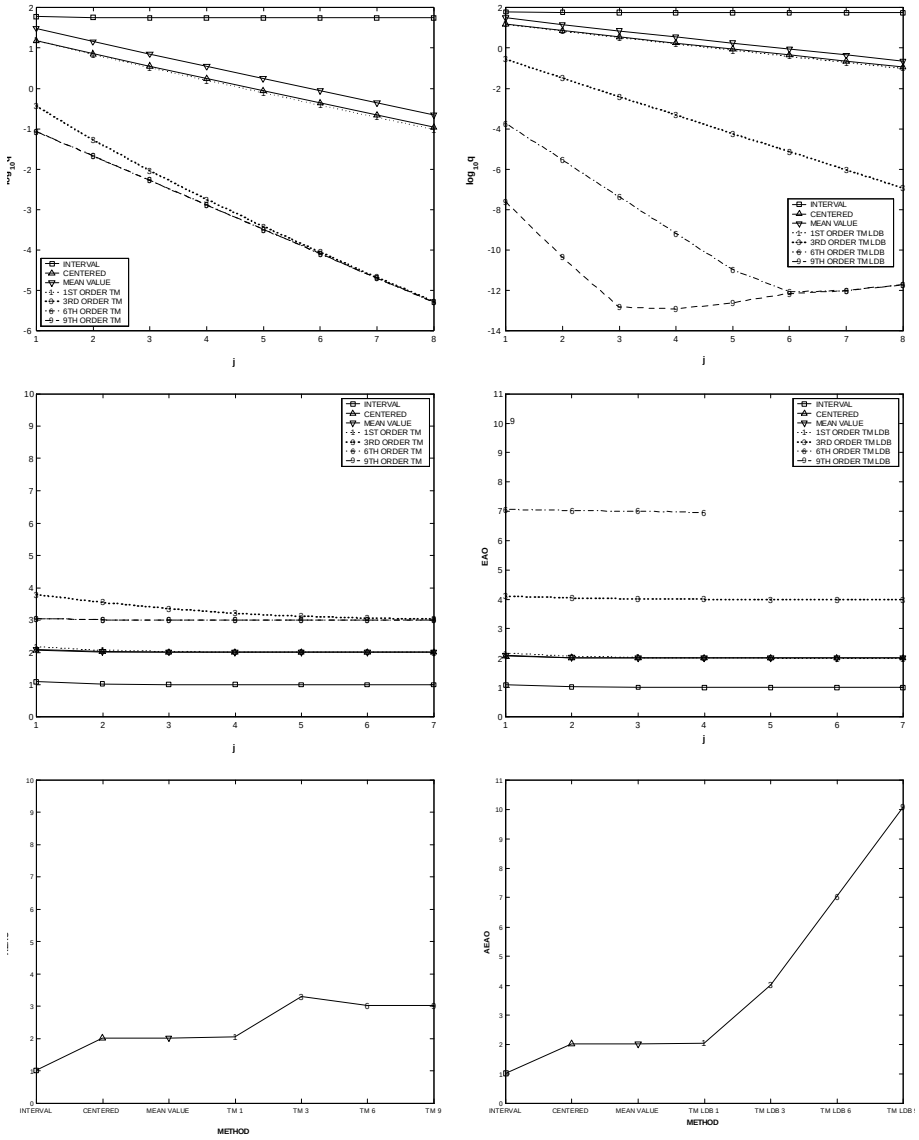

FIGURE 7. At the expansion point $x_0 = 3\pi/2$.

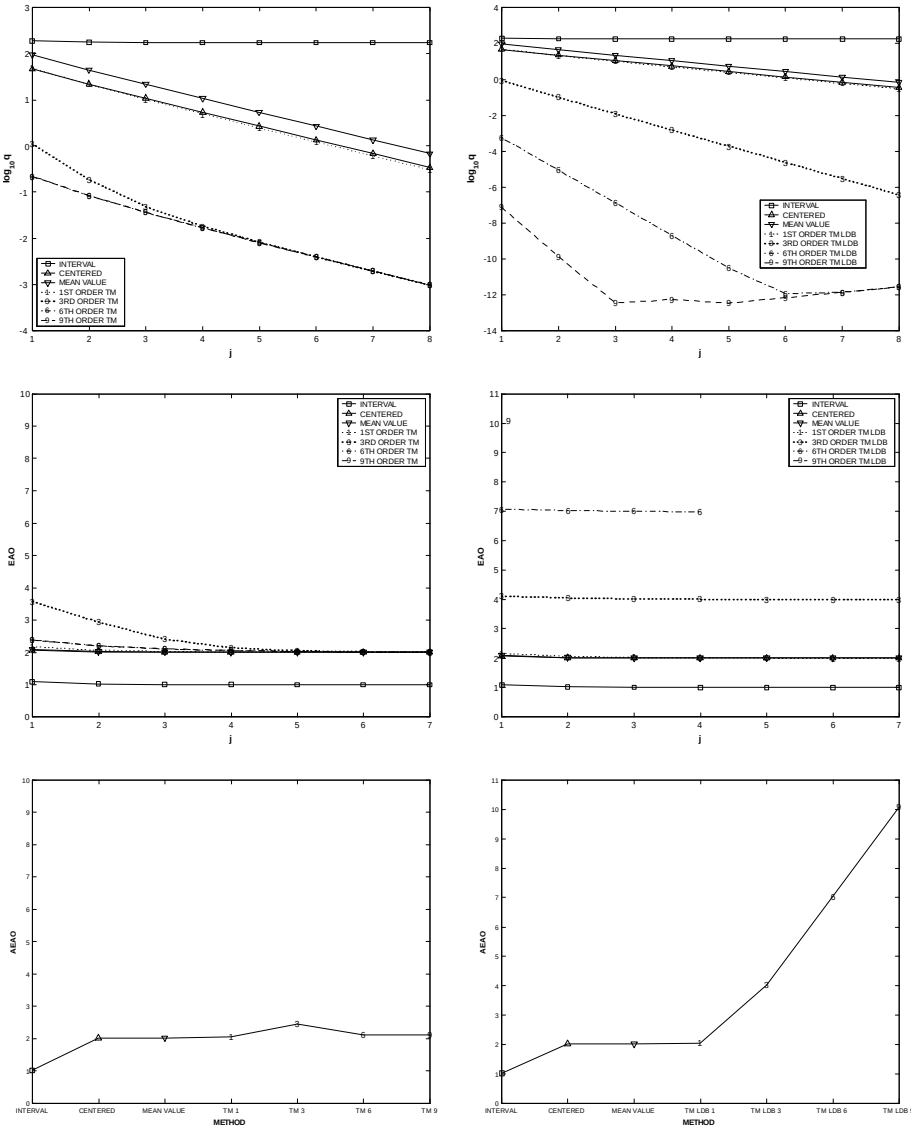

FIGURE 8. At the expansion point $x_0 = 7\pi/4$.

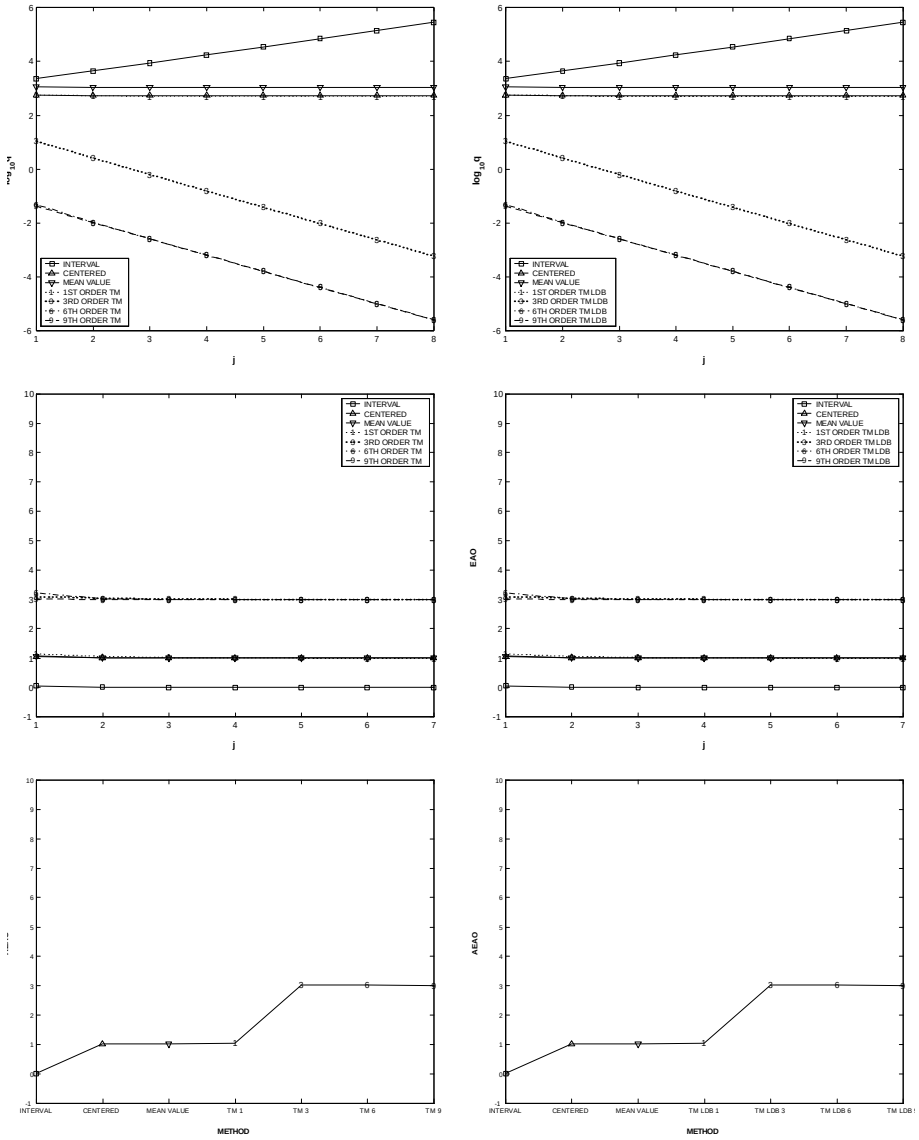

FIGURE 9. At the expansion point $x_0 = 2\pi$.

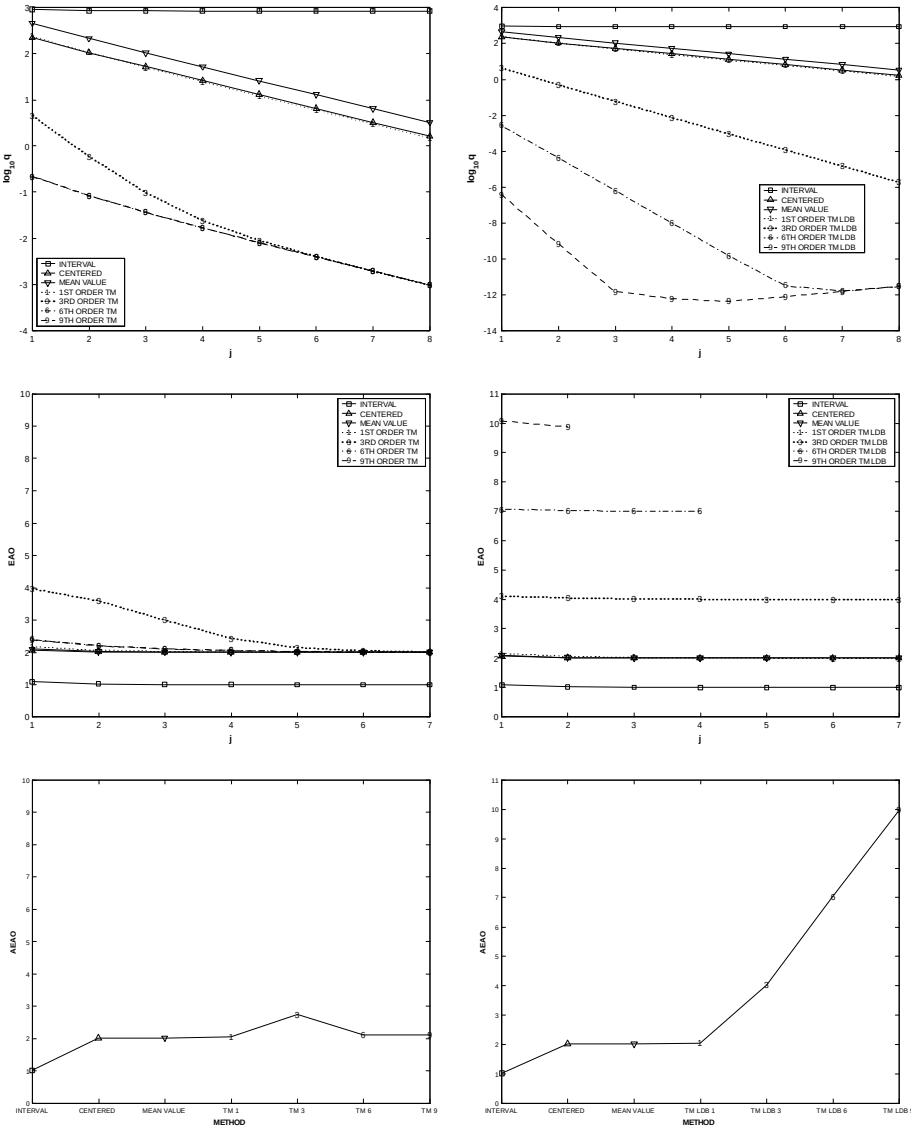

FIGURE 10. At the expansion point $x_0 = 9\pi/4$.

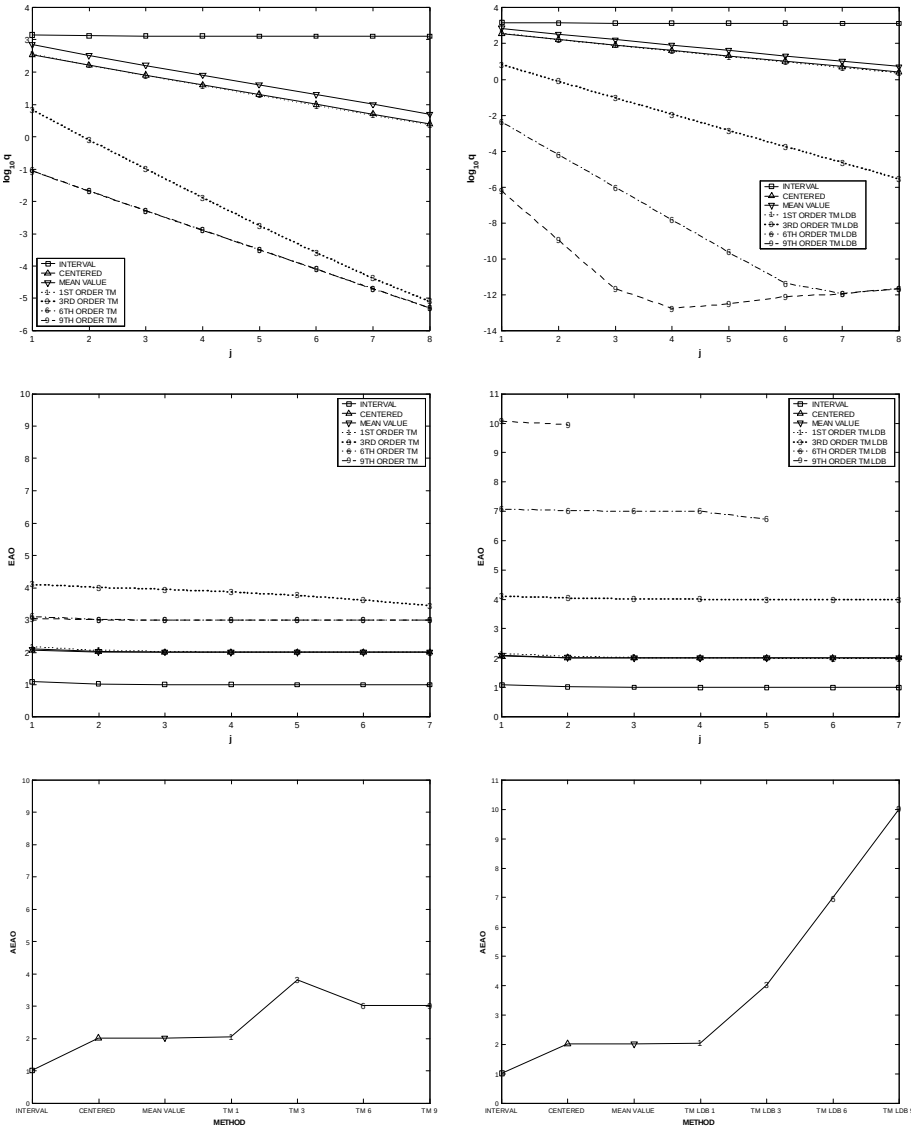

FIGURE 11. At the expansion point $x_0 = 5\pi/2$.

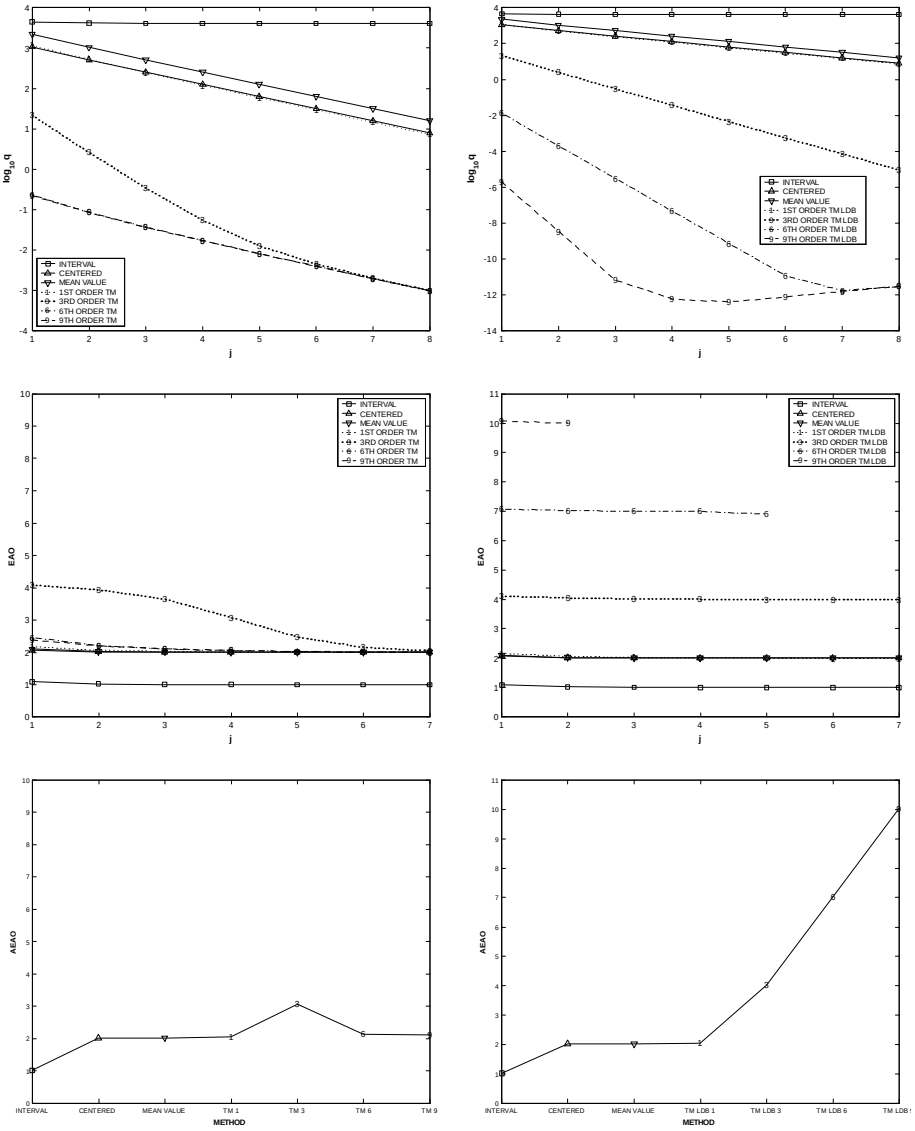

FIGURE 12. At the expansion point $x_0 = 11\pi/4$.

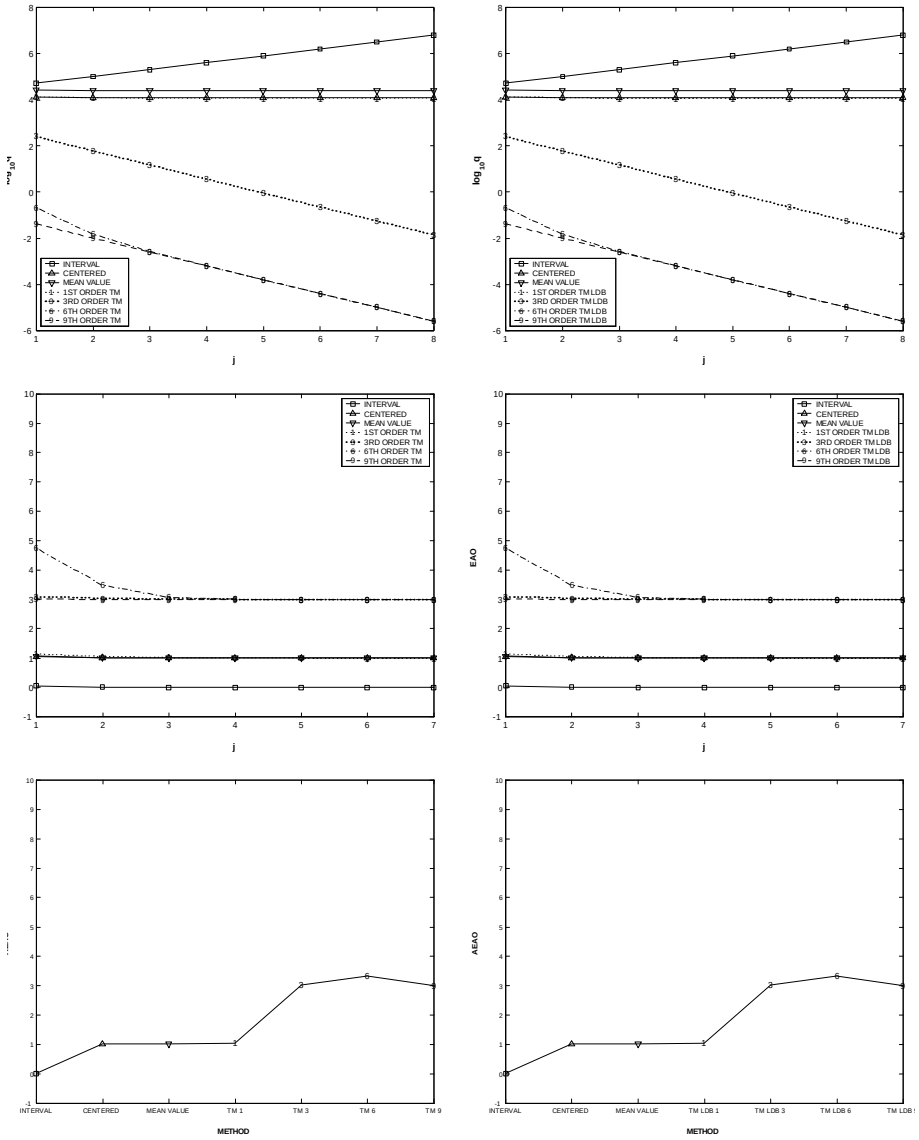

FIGURE 13. At the expansion point $x_0 = 3\pi$.

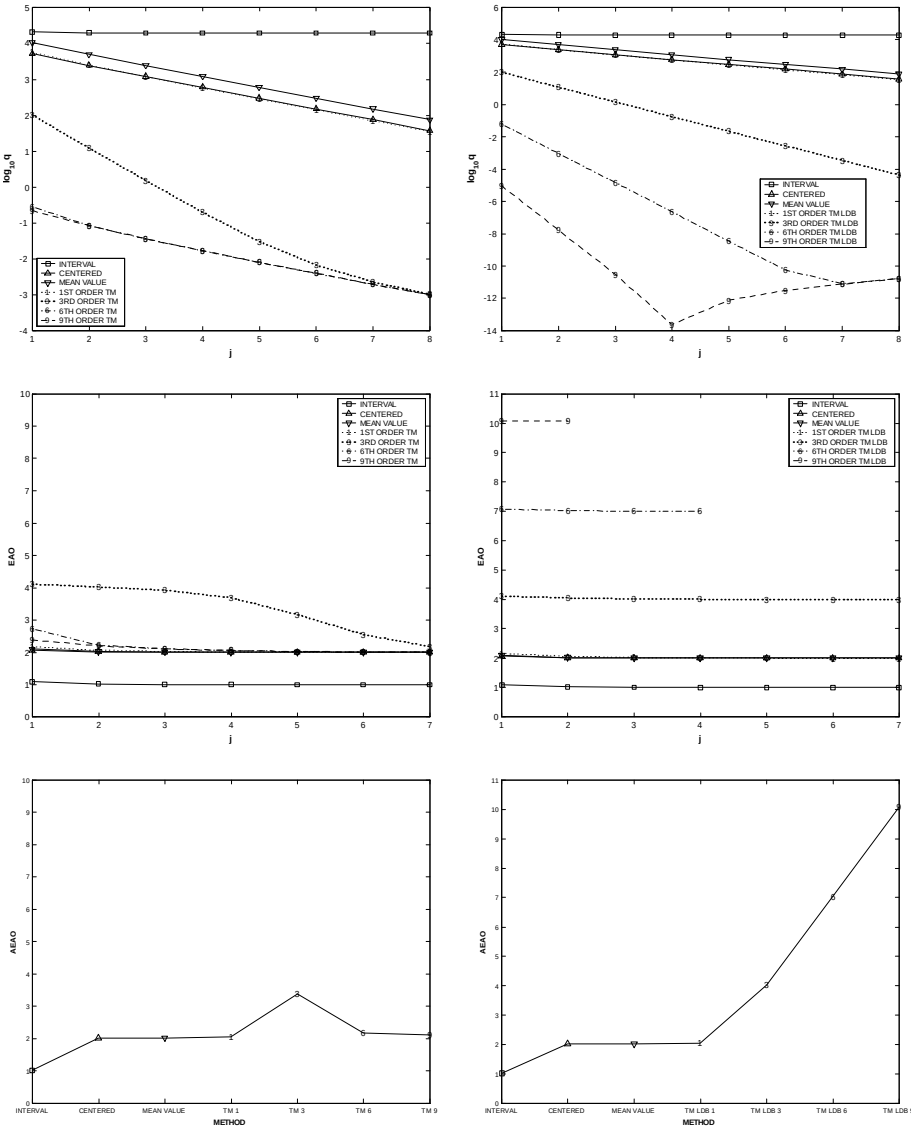

FIGURE 14. At the expansion point $x_0 = 13\pi/4$.

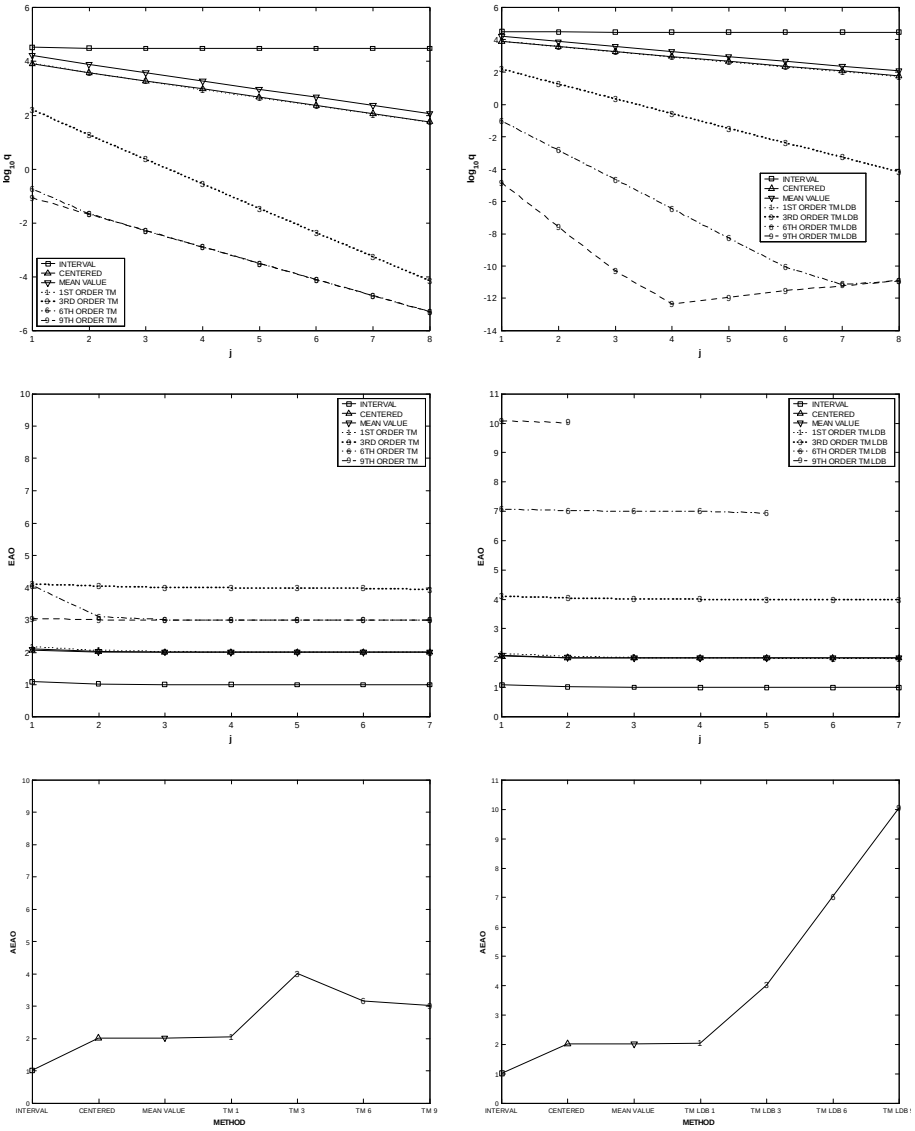

FIGURE 15. At the expansion point $x_0 = 7\pi/2$.

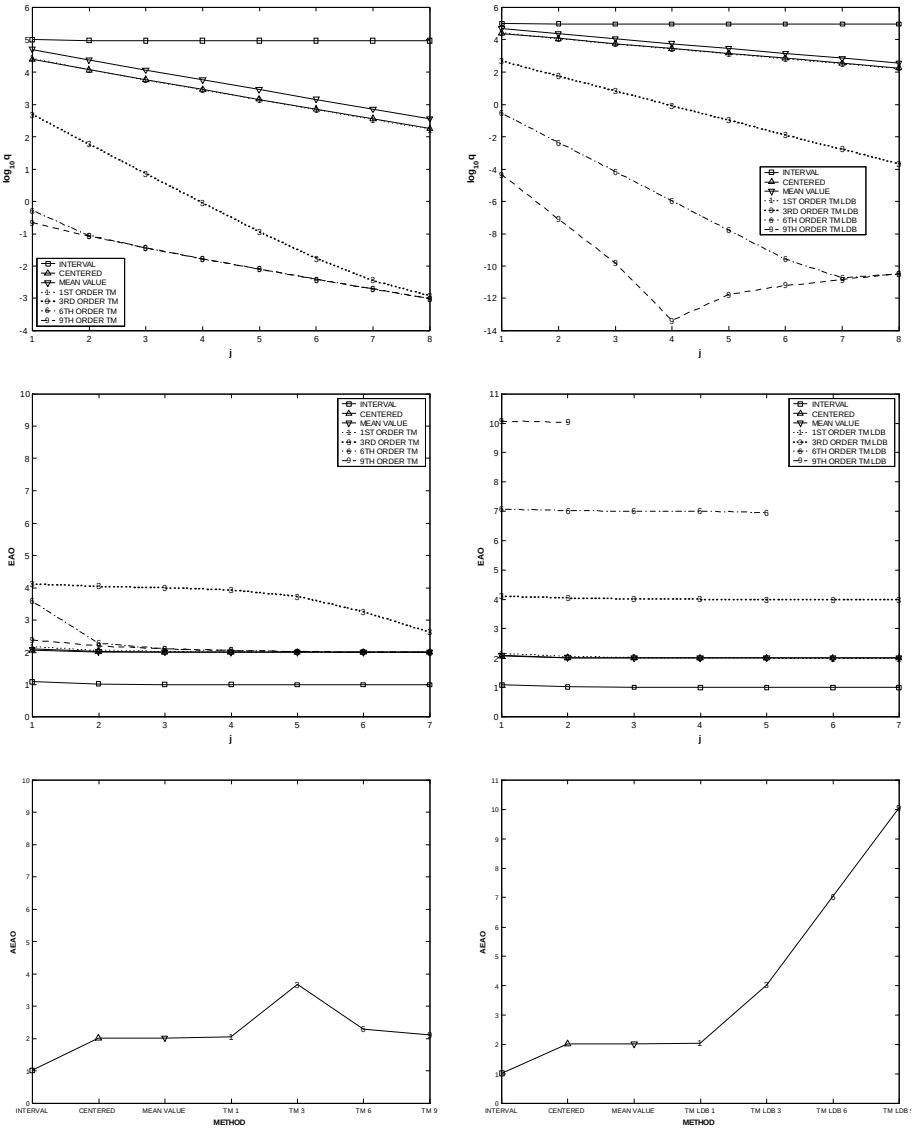

FIGURE 16. At the expansion point $x_0 = 15\pi/4$.

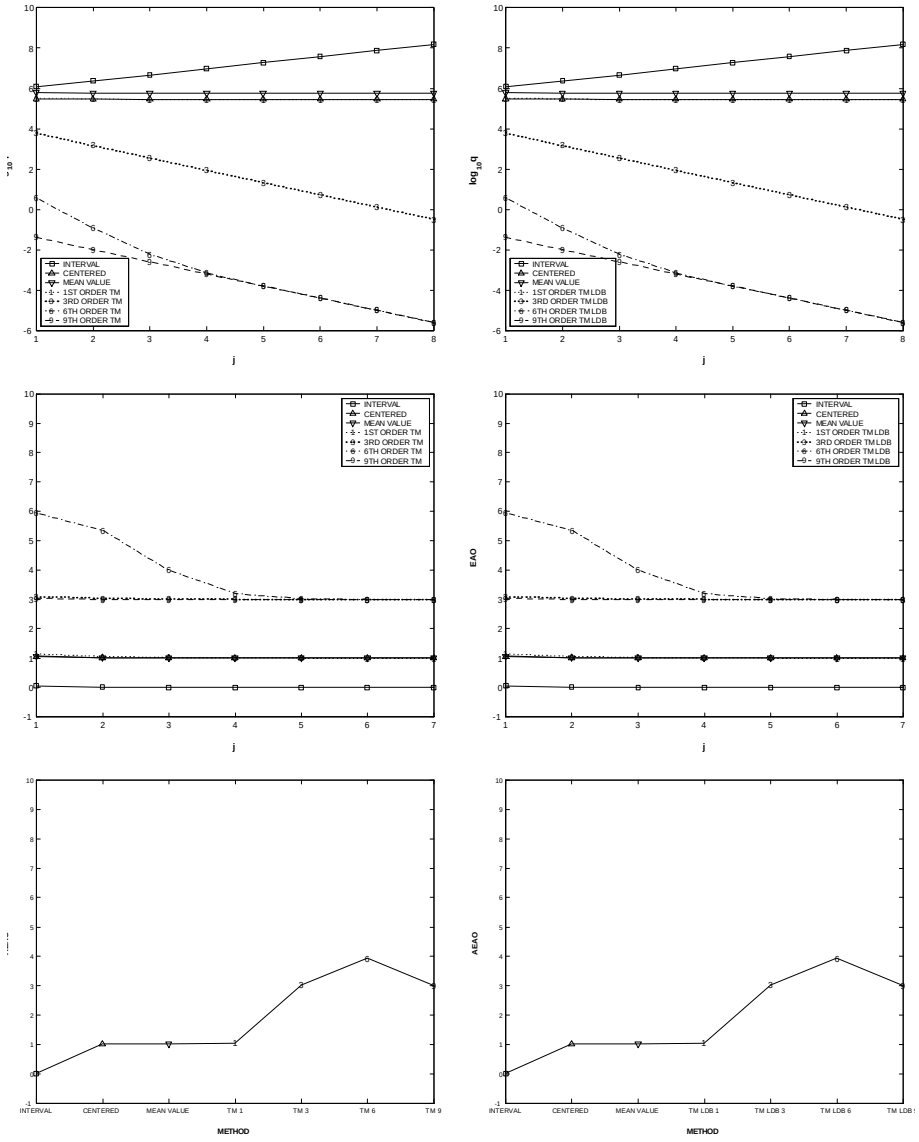

FIGURE 17. At the expansion point $x_0 = 4\pi$.